Intrinsic Paramagnetic Meissner Effect Due to *s*-Wave Odd-Frequency Superconductivity

A. Di Bernardo,[1] Z. Salman,[2] X. L. Wang,[3] M. Amado,[1] M. Egilmez,[4] M. G. Flokstra,[5] A. Suter,[2] S. L. Lee,[5] J. H. Zhao,[3] T. Prokscha,[2] E. Morenzoni,[2] M. G. Blamire,[1] J. Linder,[6] and J. W. A. Robinson[1,*]

[1]*Department of Materials Science and Metallurgy, University of Cambridge, 27 Charles Babbage Road, Cambridge CB3 0FS, United Kingdom*
[2]*Laboratory for Muon Spectroscopy, Paul Scherrer Institute, 5232 Villigen PSI, Switzerland*
[3]*State Key Laboratory of Superlattices and Microstructures, Institute of Semiconductors, Chinese Academy of Sciences, Beijing 100083, China*
[4]*Department of Physics, American University of Sharjah, Sharjah 26666, United Arab Emirates*
[5]*School of Physics and Astronomy, SUPA, University of St. Andrews, St. Andrews KY16 9SS, United Kingdom*
[6]*Department of Physics, Norwegian University of Science and Technology, N-7491 Trondheim, Norway*

(Received 14 July 2015; published 6 November 2015)

In 1933, Meissner and Ochsenfeld reported the expulsion of magnetic flux—the diamagnetic Meissner effect—from the interior of superconducting lead. This discovery was crucial in formulating the Bardeen-Cooper-Schrieffer (BCS) theory of superconductivity. In exotic superconducting systems BCS theory does not strictly apply. A classical example is a superconductor-magnet hybrid system where magnetic ordering breaks time-reversal symmetry of the superconducting condensate and results in the stabilization of an odd-frequency superconducting state. It has been predicted that under appropriate conditions, odd-frequency superconductivity should manifest in the Meissner state as fluctuations in the sign of the magnetic susceptibility, meaning that the superconductivity can either repel (diamagnetic) or attract (paramagnetic) external magnetic flux. Here, we report local probe measurements of faint magnetic fields in a Au/Ho/Nb trilayer system using low-energy muons, where antiferromagnetic Ho (4.5 nm) breaks time-reversal symmetry of the proximity-induced pair correlations in Au. From depth-resolved measurements below the superconducting transition of Nb, we observe a local enhancement of the magnetic field in Au that exceeds the externally applied field, thus proving the existence of an intrinsic paramagnetic Meissner effect arising from an odd-frequency superconducting state.

DOI: 10.1103/PhysRevX.5.041021

Subject Areas: Condensed Matter Physics, Magnetism, Superconductivity

I. INTRODUCTION

Below the superconducting transition of a conventional (*s*-wave) Bardeen-Cooper-Schrieffer (BCS) superconductor such as Nb, the electrons stabilize into Cooper pairs in a spin-singlet state, meaning that the electrons of a pair have oppositely aligned spins. The screening supercurrent density ($\boldsymbol{J}$) that is generated by a superconductor in response to a weak magnetic field is linearly proportional to the vector potential ($\boldsymbol{A}$) via the density of pairs present n_s ($\boldsymbol{J} = -e^2 n_s \boldsymbol{A}/mc$, where c, e, and m are the speed of light, the electron charge, and the electron rest mass, respectively). Consequently, the amplitude of the screening supercurrent density (J) is negative and a diamagnetic Meissner effect is observed [1].

The opposite effect—the attraction of magnetic flux—has also been observed in superconductors [2–5], but this paramagnetic Meissner effect is metastable and is due to inhomogeneities and is not, therefore, intrinsic to the superconductivity. An intrinsic paramagnetic Meissner state has been predicted in *s*-wave superconductors with broken time-reversal symmetry, as a result of an emergent unconventional odd-frequency superconducting state, which competes with conventional (even-frequency) superconductivity (see [6–9] and related theory in [10]).

At the surface of an *s*-wave superconductor proximity coupled to a magnetic metal, the exchange field of the magnet can induce an odd-frequency superconducting state in which the Cooper pairs are in a spin-triplet state with a density (n_t) that is a mixture of spin-zero and spin-one pair projections [11–13]. This means that $\boldsymbol{J}$ is dependent on the magnitude and sign of $n_s - n_t$ [i.e., $\boldsymbol{J} = -e^2(n_s - n_t)\boldsymbol{A}/mc$] [14] and so odd-frequency triplets should act to reduce the screening current [6]. Since n_s and n_t have different decay envelopes in an exchange field, $\boldsymbol{J}$ should reverse in sign as a function of magnetic layer thickness when n_t exceeds n_s, at which point the magnetic susceptibility is positive and an inverse—paramagnetic—Meissner effect [6–9] prevails.

*Corresponding author.
jjr33@cam.ac.uk

Evidence for spin-triplet pairing has recently been demonstrated in experimental studies involving magnetically inhomogeneous superconductor/ferromagnet (S/F) hybrids, such as via transition temperature measurements of S/F1/F2 spin valves [15], long-ranged supercurrents in S/F/S Josephson junctions [16], and various spectroscopy measurements on F/S systems [17].

To investigate the Meissner effect in a superconductor-magnet system, we measure the depth profile of the local magnetic susceptibility of a Au(27.5 nm)/Ho(4.5 nm)/Nb(150 nm) trilayer by low-energy muon spin spectroscopy (LE-μSR). The antiferromagnetic rare-earth metal Ho breaks time-reversal symmetry of the pair correlations in Au and has a thickness that is comparable to the known coherence length for singlet pairs in Ho [18] to ensure pair transmission into Au. The Au layer is necessary since a Meissner state cannot be probed by muons directly in a magnetic material due to their rapid depolarization in a strong magnetic field. Here, we report the discovery of the paramagnetic Meissner effect in Au, which is found to be an intrinsic property of the odd-frequency superconducting state that is generated via the superconductor proximity effect.

II. RESULTS

LE-μSR offers extreme sensitivity to magnetic fluctuations and spontaneous fields of less than 0.1 G with a depth-resolved sensitivity of a few nanometers [19–23]. To probe the depth dependence [z coordinate in Fig. 1(a)] of the Meissner response in Au/Ho/Nb by LE-μSR, an external field ($B_{\rm ext}$) is applied parallel to the sample plane [along the y coordinate in Fig. 1(a)] and perpendicular to the muon initial spin polarization (oriented in the x-z plane), as sketched in Fig. 1(a). The muon spin polarization is proportional to the asymmetry of decay positrons from the implanted muons as shown in Fig. 1(b), which is experimentally determined as a difference in the number of counting events of the two detectors, as discussed in the Supplemental Material [24].

In this transverse-field configuration, a muon's spin polarization precesses on average at a frequency

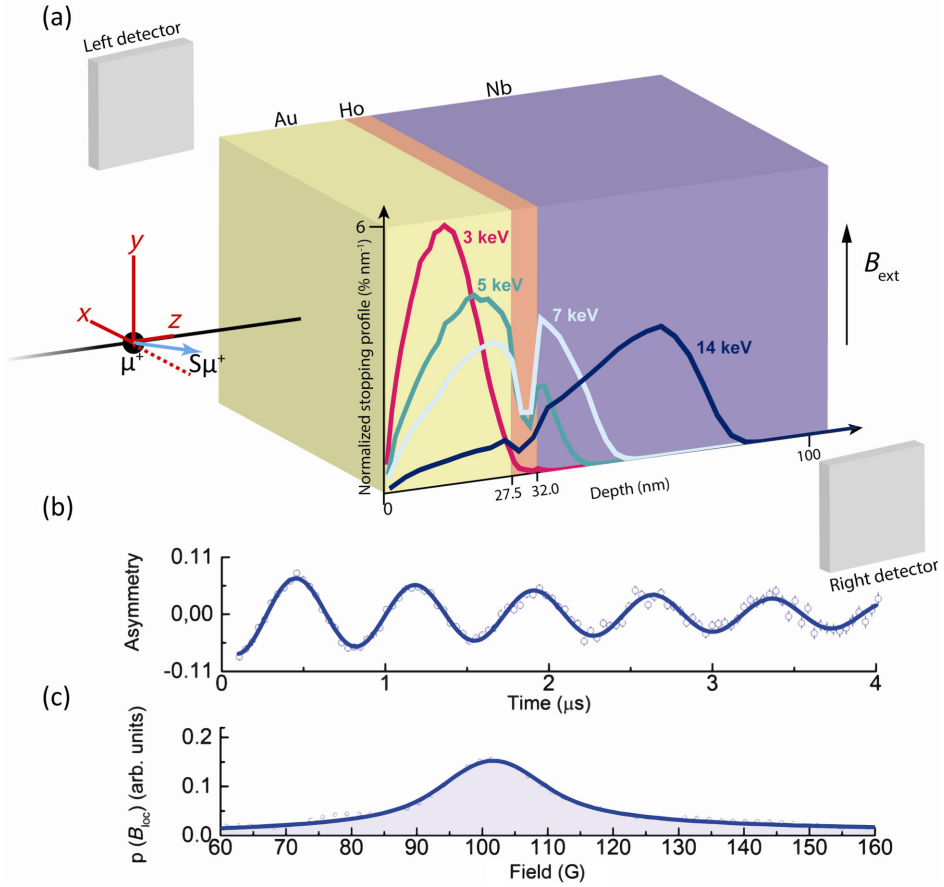

FIG. 1. Simulated muon stopping distributions in Au/Ho/Nb. (a) Experimental LE-μSR setup in transverse-field configuration and normalized muon stopping profiles $p(z, E)$ in Au/Ho/Nb simulated for a few representative implantation energies E. (b) Experimental asymmetry data determined from the counting events of the positron detectors for muons implanted in Au/Ho/Nb with $E = 4.5$ keV at 3 K (blue dots) and single-energy asymmetry fit (blue curve). (c) Fourier transform of the asymmetry in (b), which represents the magnetic-field distribution.

$\bar{\omega}_s = \gamma_\mu \bar{B}_{\rm loc}$ about the average local field $\bar{B}_{\rm loc}$ sensed by the implanted muons, with $\gamma_\mu = 2\pi * 135.5$ MHz T^{-1} being the muon gyromagnetic ratio. Assuming a local field profile $B_{\rm loc}(z)$ within the sample, muons implanted with energy E and a corresponding stopping distribution $p(z,E)$ precess at an average frequency $\bar{\omega}_s = \gamma_\mu \bar{B}_{\rm loc} = \gamma_\mu \int B_{\rm loc}(z) p(z,E) dz$ [25]. The asymmetry spectrum $A_s(t,E)$ is proportional to $e^{-\bar{\lambda}t}\cos[\gamma_\mu \bar{B}_{\rm loc} t + \varphi_0(E)]$ for each implantation energy E [$\bar{\lambda}$ and $\varphi_0(E)$ being the mean depolarization rate and starting phase of the muon precession, respectively]. The experimental $B_{\rm loc}(z)$ profile is therefore sampled as a series of mean-field values $\bar{B}_{\rm loc}$ of the magnetic-field distributions $p(B_{\rm loc})$ [Fig. 1(c)] determined as fits of the corresponding asymmetry functions $A_s(t,E)$ measured at different energies E [24].

To investigate the paramagnetic Meissner effect, implantation energies in the 3–6 keV range are used to determine the $B_{\rm loc}(z)$ profile in the Au layer. At the lowest energy of 3 keV, the muons contributing to the asymmetry stop within the Au, while for increasing energy, an increasing fraction stops within the Ho and Nb layers [Fig. 1(a) and Fig. S1 in the Supplemental Material [24]]. The implantation profiles are calculated using the Monte Carlo algorithm TrimSP [26]. To minimize the contribution from backscattered muons [26] to the measured signal, implantation energies below 3 keV are not used. For muon energies above ~7 keV, the contribution of the Nb becomes dominant and therefore not relevant for probing the Meissner state in the Au (Fig. S1 [24]). However, energies above 7 keV are important to confirm the emergence of a conventional (diamagnetic) Meissner response in Nb in the superconducting state. Muons stopping in the Ho layer depolarize almost immediately and do not contribute to the measured asymmetry.

Figures 2(a) and 2(b) show the $\bar{B}_{\rm loc}$ values as a function of implantation energy, obtained from fits to the data in the normal state at $T = 10$ K and in the superconducting state at $T = 5$ K (the critical temperature T_c is ~8.52 K for the multilayer as reported in Fig. S2 of the Supplemental

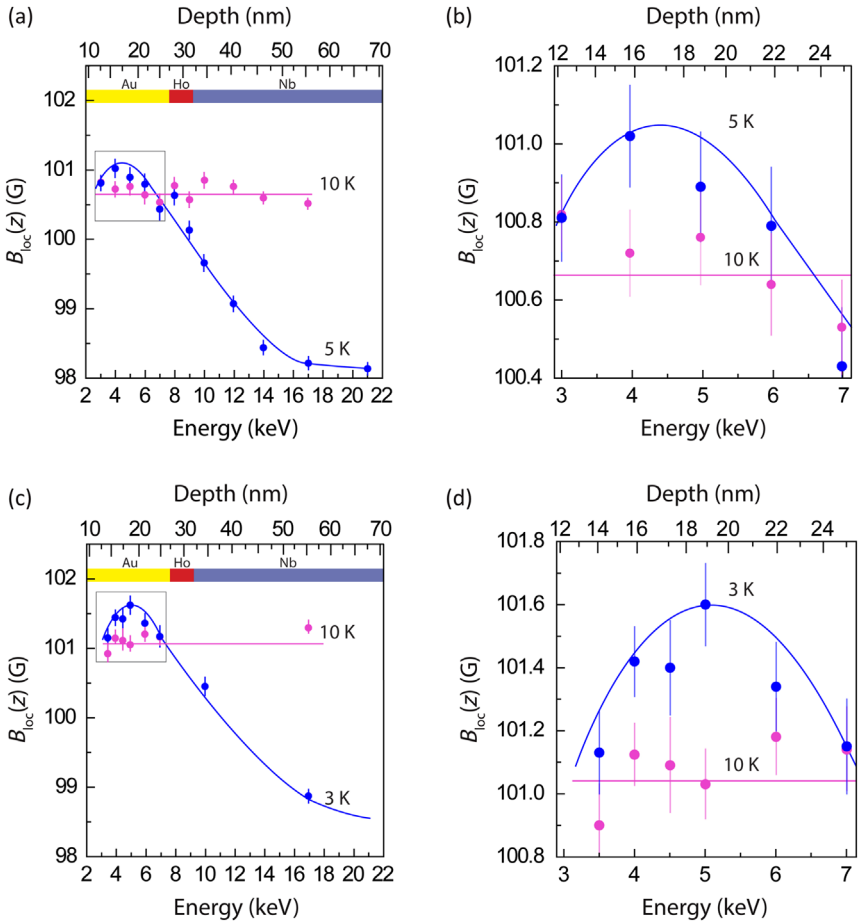

FIG. 2. Average local magnetic field in Au/Ho/Nb as a function of the muon implantation energy and mean stopping distance. (a) $\bar{B}_{\rm loc}$ values from single-energy asymmetry fits versus implantation energy (bottom x axis) and mean stopping distance (top x axis) in the normal state (magenta circles 10 K) and superconducting state (blue circles 5 K), and in (b) identical data showing the inverse Meissner state in Au. The continuous lines are a guide to the eye. (c),(d) Remeasured data after warming and cooling, but the superconducting state is now measured at 3 K.

Material [24]). Figures 2(c) and 2(d) show similar plots but following warming and recooling with data taken at $T = 10$ K and $T = 3$ K; 6×10^6 positron-counting events were collected per datum point. The average stopping depth $\bar{z}(E)$ of the muon stopping profiles $p(z, E)$ for the corresponding implantation energy E are plotted on the top axes in Fig. 2. The nonlinearity of these depth scales stems from the fact that $\bar{z}(E)$ does not increase proportionally with E, as shown in Fig. S1(b) of the Supplemental Material [24]. Since the two energy scans at 3 and 5 K are performed at different stages, the normal-state (10 K) energy scan is reacquired to avoid any influence on the measurement data from the specific magnetic configuration reached by Ho after cooling through its magnetic transitions.

The normal-state (10 K) data in Fig. 2 show that $\bar{B}_{\mathrm{loc}}$ is approximately depth independent and closely matches the externally applied field value B_{ext} of about 101 G [magenta curves in Figs. 2(a) and 2(c)]. The superconducting-state data (5 and 3 K), however, show a more complex behavior. In Nb, the local field decreases as a function of depth in Nb and, for both temperatures, reaches a flux expulsion of about 2.5 G for the 17-keV scan [corresponding to $\bar{z} \sim 29.7$ nm from the Ho/Nb interface as shown in Fig. S1(b) in the Supplemental Material [24]], consistent with conventional diamagnetic Meissner screening. In contrast, the opposite behavior is observed in Au. Here, the local field increases by about 0.5 G at $T = 3$ K and about 0.25 G at $T = 5$ K above the applied field [and, therefore, the normal-state value of $B_{\mathrm{loc}}(z)$], indicating a paramagnetic screening where $B_{\mathrm{loc}}(z)$ appears nonmonotonic with depth [blue curves in Figs. 2(a) and 2(c)]. We note that comparative LE-μSR studies by Morenzoni *et al.* on normal metal/Nb (N/Nb) bilayers demonstrate a purely diamagnetic response in the normal metal in the superconducting state, as expected due to the absence of a magnetic interface [27]. Although the measured increase in the local field $\Delta B_{\mathrm{loc}}(z)$ in the superconducting state relative to the normal state is small, it exceeds the statistical and systematic measurement error in $B_{\mathrm{loc}}(z)$ (error bars in Fig. 2). Furthermore, $\Delta B_{\mathrm{loc}}(z)$ increases at lower temperatures, which implies that the magnitude of $\Delta B_{\mathrm{loc}}(z)$ is related to the amplitude of the superconducting order parameter, which is consistent with theory [7,8].

Although the asymmetry fits for single implantation energy in Fig. 2 show a paramagnetic Meissner effect in Au below the Nb superconducting transition, the $B_{\mathrm{loc}}(z)$ profiles obtained with this approach include depth averaging due to the width of muon stopping distributions. To obtain an accurate $B_{\mathrm{loc}}(z)$ profile, a global fit for all implantation energies with a common field profile is used [19–23]. The common field profile in the Au layer is modeled as $B_{\mathrm{loc}}(z) = B_{\mathrm{ext}} + M(z)$, where we set the magnetization term to $M(z) = B_a \sin(z/\kappa)$, which is a parametrization of the theoretical magnetization profile calculated for the Au/Ho/Nb heterostructure.

The theoretical magnetization is computed from the vector potential $\boldsymbol{A}$ determined as a solution of the Maxwell equation $(d^2\boldsymbol{A}/dz^2) = -\boldsymbol{J} = -J_x(z)\boldsymbol{A}$, where the supercurrent $\boldsymbol{J}$ is assumed proportional to the vector potential $\boldsymbol{A}$ via the term $J_x(z)$ including the dependence on the anomalous Green's function (see Supplemental Material [24]). In this expression, $J_x(z)$ also represents the component of the supercurrent density $\boldsymbol{J}$ along the x axis in Fig. 1(a). Both odd-frequency and even-frequency pairing correlations contribute to $\boldsymbol{J}$, which is calculated using the quasiclassical theory of superconductivity under the assumption that time-reversal symmetry is spontaneously broken by the spatially dependent exchange field of the Ho, which forms a conical pattern along the z coordinate in Fig. 1(a). We also take into account the spin-selective scattering taking place at the interface between Nb and Ho by using spin-dependent boundary conditions [24]. Our model excludes the presence of a Fulde-Ferrel-Larkin-Ovchinnokov state, which can theoretically compete with the paramagnetic Meissner state, but only if the superconducting layer is thinner than the magnetic screening length [6]. In Nb the magnetic screening length is about 90 nm, which is much shorter than the thickness of the Nb used here of 150 nm, and so contributions from the Fulde-Ferrel-Larkin-Ovchinnokov state can be ignored, as stated in Ref. [6].

In a normal metal (N) proximity coupled to a superconductor (S), only even-frequency pairing correlations contribute to the screening supercurrent induced in N. The theoretical $M(z)$ profile in this case is $\propto \cosh(kz)/\cosh(k)$ (k being a measure for the supercurrent magnitude depending on several parameters, including the thickness of the S/N bilayer, the diffusion constants, and the superconducting gap; for details see Supplemental Material [24]), which represents a monotonic decay from the S/N interface as expected for a conventional (diamagnetic) Meissner effect. In the presence of additional odd-frequency pairing correlations in the screening supercurrent induced by a magnetically active layer separating the S/N interface (Ho in our case) instead, $B_{\mathrm{loc}}(z)$ in N shows an oscillatory behavior about B_{ext} assuming both positive and negative values. In the particular case of Au/Ho/Nb, using realistic values for the physical parameters involved in the description of the proximity effect occurring in Au and Ho, the expected theoretical profile for $B_{\mathrm{loc}}(z)$ shows a single oscillation reaching a maximum inside Au (blue curve in Fig. 3). Therefore, also making the realistic assumption that $B_{\mathrm{loc}}(z)$ matches the applied external field B_{ext} at the Au-vacuum interface, it is clear that $B_{\mathrm{loc}}(z) = B_{\mathrm{ext}} + B_a \sin(z/\kappa)$ represents an appropriate parametrization of the oscillatory local magnetic-field profile in Au to use in the global energy fit. This parametrization is also in agreement with the experimental profiles determined at 3 and 5 K by sampling $B_{\mathrm{loc}}(z)$ at different energies, which can be approximated by half-period sine functions (blue curves for Au in Fig. 2).

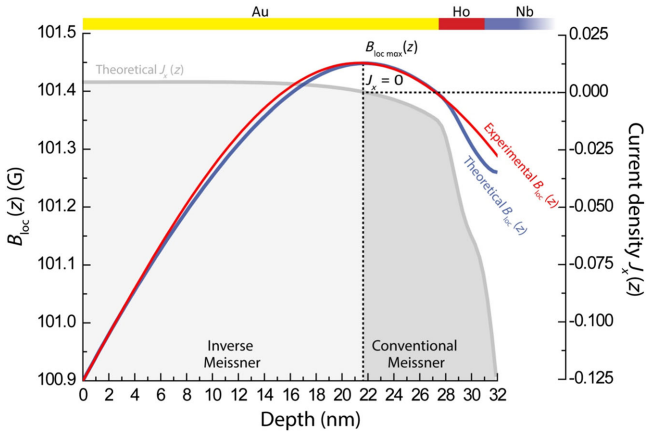

FIG. 3. Magnetization and screening current profile from the Ho/Nb interface in Au/Ho/Nb. Local magnetic field $B_{\rm loc}(z)$ determined as global-energy fit of the LE-μSR measurement data (red curve, left y axis) and theoretical model (blue curve, left y axis); calculated dimensionless screening current density $J_x(z)$ flowing parallel to the x axis in Fig. 1(a) inside the plane of the thin film heterostructure (gray curve, right y axis). Dashed lines show that the position of the maximum in $B_{\rm loc}(z)$ coincides with that of the null in $J_x(z)$.

The global energy fit is implemented on the measurement data at 3 K, which show the most significant paramagnetic Meissner response in Au. An exponential depolarization function $G(t,E) = e^{-\bar{\lambda}t}$ is used for the fit, with $\bar{\lambda}$ being a fitting parameter common for all energies [24]. In the analytic expression for $B_{\rm loc}(z)$, $B_{\rm ext}$ is set equal to the normal-state field obtained from the global fit of the measurement data at 10 K under the assumption that $B_{\rm loc}(z)$ can be modeled as a constant field at this temperature [magenta curve in Fig. 2(c)]. Figure 3 illustrates the results of the global fit at 3 K, which verify a positive increase of $B_{\rm loc}(z)$ in Au over $B_{\rm ext}$. The chi-square minimization algorithm reported good convergence (chi-square/numbers of degrees of freedom $= 1.072$) yielding $B_a = 0.55$ G and $\bar{\lambda} = 0.229\ \mu{\rm s}^{-1}$ as optimal fitting parameters. The parameter κ is kept fixed and equal to 13.58 nm to match the position of the peak in the $B_{\rm loc}(z)$ theoretical profile.

The $B_{\rm loc}(z)$ profile obtained with these values for $\bar{\lambda}$, B_a, and κ (red curve in Fig. 3) is in good agreement with the theoretical $B_{\rm loc}(z)$ curve (blue curve in Fig. 3), thus validating the good convergence of the algorithm and the appropriateness of the parametric model used for the fitting. In addition, even when κ is allowed to vary, the fits converge to a κ value that is not significantly different ($\sim$15.2 nm), while B_a remains the same, attesting further to the appropriateness of the model.

III. DISCUSSION

While the fits to the data are in close agreement with the predicted paramagnetic Meissner effect, we first rule out other possibilities that could lead to an increase in magnetic flux in Au. However, as we discuss below, none of these should show temperature dependence in the measured range of 3–10 K. One mechanism that can result in a magnetization enhancement in Au is Ruderman-Kittel-Kasuya-Yosida (RKKY)-type oscillations in the spin polarization of Au induced via an interaction with Ho. The largest period predicted [28] and reported experimentally [29] for RKKY oscillations in epitaxial Au (001) is 7–8 monolayers or $\sim$1.6 nm, which is much too small to explain the behavior observed in Fig. 2, where the oscillation period of the magnetization exceeds several tens of nanometers. Furthermore, RKKY oscillations should also lead to an additional broadening of the magnetic-field distribution experienced by muons (other than to the measured shift in average field) [30] and also be present in the normal-state data at 10 K, which we do not observe. A second possibility is an enhancement of the magnetization of Ho for decreasing temperature. Similarly to the case of RKKY oscillations, however, such an enhancement should only result in a broadening of the magnetic-field distribution rather than the observed shift, because the magnetic domains have a finite size and a random orientation giving a random dipolar field profile in Au.

Oscillations in the magnetic susceptibility induced by unconventional (odd-frequency) superconductivity are therefore the most likely explanation for the paramagnetic Meissner effect in Au due to the presence of Ho [6–9]. In Fig. 2 it is shown that a conventional Meissner effect is measured in Nb up to the interface with Ho, where the contribution of spin-singlet Cooper pairs to the screening supercurrent $J_x(z)$ is larger than that due to the long-ranged spin-triplet pairs (Fig. 3). Nevertheless, while spin-singlet pairs are rapidly filtered out by the exchange field in Ho, the spin-triplet pairs rotate into each other within the Ho layer [Fig. S3(a) in the Supplemental Material [24]], so that the sum of the Green's function amplitudes for spin-one and spin-zero triplet pairs follows a much slower decay in Ho compared to the Green's function amplitude for spin singlets (Fig. S3(b) [24]). This is also consistent with the trend of the density of the screening current $J_x(z)$ profile (Fig. S3(b) in the Supplemental Material [24]), which depends on the imaginary part of the anomalous Green's functions via the difference $n_s - n_t$ between spin-singlet and spin-triplet pair densities: $J_x(z)$ starts off negative in Nb (conventional Meissner state), then increases inside Ho, and it eventually becomes positive in Au, where the total contribution from the spin triplets to the screening current overtakes the singlet one.

Finally, the results in Fig. 3 demonstrate that the paramagnetic effect is strongest in Au where the odd-frequency state dominates over the singlet state. This indicates that the paramagnetic response is an intrinsic property of the odd-frequency superconducting state and that the superconductivity must therefore carry a net

magnetization. Future experiments should explore ways to harness the magnetization generated by odd-frequency superconductivity in order to explore the potential for driving magnetization-reversal processes in the superconducting state [13].

ACKNOWLEDGMENTS

The authors thank N. Banerjee for sample growth support during the initial stages of the project. J. W. A. R. acknowledges financial support from the Royal Society. J. W. A. R. and A. D. B. acknowledge financial support from the UK EPSRC through NanoDTC EP/G037221/1 and the Leverhulme Trust through an International Network Grant (No. IN-2013-033). A. D. B. also acknowledges additional financial support from the Schiff Foundation. X. L. W. and J. H. Z. acknowledge support from the MOST of China (2015CB921500). J. L. acknowledges support from the NTNU and the Norwegian Research Council Grants (No. 205591, No. 216700, No. 240806). J. L., J. W. A. R., and A. D. B. also acknowledge support from the COST Action MP-1201 "Novel Functionalities through Optimized Confinement of Condensate and Fields." S. L. L. and M. G. F. acknowledge the support of the EPSRC through Grant No. EP/J01060X. The muSR measurements were performed at the Swiss Muon Source (SμS), at the Paul Scherrer Institute in Villigen, Switzerland. The project has also received funding from the European Union's Seventh Framework Programme for research, technological development and demonstration under the NMI3-II Grant No. 283883. Data accompanying this publication are directly available at https://www.repository.cam.ac.uk/handle/1810/251382 data repository.

[1] W. Meissner and R. Ochsenfeld, *Ein neuer Effect bei Eintritt der Supraleitfähigkeit*, Naturwissenschaften **21**, 787 (1933).

[2] W. Braunisch, N. Knauf, V. Kataev, S. Neuhausen, A. Grütz, A. Kock, B. Roden, D. Khomskii, and D. Wohlleben, *Paramagnetic Meissner Effect in Bi High-Temperature Superconductors*, Phys. Rev. Lett. **68**, 1908 (1992).

[3] P. Svelindh, K. Niskanen, P. Norling, P. Nordblad, L. Lundgren, B. Lönnberg, and T. Lundström, *Anti-Meissner Effect in the BiSrCaCuO System*, Physica (Amsterdam) **162–164C**, 1365 (1989).

[4] D. J. Thompson, M. S. M. Minhaj, L. E. Wenger, and J. T. Chen, *Observation of Paramagnetic Meissner Effect in Niobium Disks*, Phys. Rev. Lett. **75**, 529 (1995).

[5] A. K. Geim, S. V. Dubonos, J. G. S. Lok, M. Henini, and J. C. Maan, *Paramagnetic Meissner Effect in Small Superconductors*, Nature (London) **396**, 144 (1998).

[6] S. Mironov, A. Mel'nikov, and A. Buzdin, *Vanishing Meissner Effect as a Hallmark of In-Plane Fulde-Ferrell-Larkin-Ovchinnikov Instability in Superconductor-Ferromagnet Layered Systems*, Phys. Rev. Lett. **109**, 237002 (2012).

[7] M. Alidoust, K. Halterman, and J. Linder, *Meissner Effect Probing of Odd-Frequency Triplet Pairing in Superconducting Spin Valves*, Phys. Rev. B **89**, 054508 (2014).

[8] T. Yokoyama, Y. Tanaka, and N. Nagaosa, *Anomalous Meissner Effect in a Normal-Metal-Superconductor Junction with a Spin-Active Interface*, Phys. Rev. Lett. **106**, 246601 (2011).

[9] F. S. Bergeret, A. F. Volkov, and K. B. Efetov, *Josephson Current in Superconductor-Ferromagnet Structures with a Nonhomogeneous Magnetization*, Phys. Rev. B **64**, 134506 (2001).

[10] F. S. Bergeret, A. F. Volkov, and K. B. Efetov, *Induced Ferromagnetism Due to Superconductivity in Superconductor-Ferromagnet Structures*, Phys. Rev. B **69**, 174504 (2004); F. S. Bergeret, A. L. Yeyati, and A. Martin-Rodero, *Inverse Proximity Effect in Superconductor-Ferromagnet Structures: From the Ballistic to the Diffusive Limit*, Phys. Rev. B **72**, 064524 (2005); F. S. Bergeret and N. Garcia, *Spin Screening and Antiscreening in a Ferromagnet/Superconductor Heterojunction*, Phys. Rev. B **70**, 052507 (2004).

[11] F. S. Bergeret, A. F. Volkov, and K. B. Efetov, *Enhancement of the Josephson Current by an Exchange Field in Superconductor-Ferromagnet Structures*, Phys. Rev. Lett. **86**, 3140 (2001).

[12] F. S. Bergeret, A. F. Volkov, and K. B. Efetov, *Odd Triplet Superconductivity and Related Phenomena in Superconductor-Ferromagnet Structures*, Rev. Mod. Phys. **77**, 1321 (2005).

[13] J. Linder and J. W. A. Robinson, *Superconducting Spintronics*, Nat. Phys. **11**, 307 (2015).

[14] Y. Asano, A. A. Golubov, Y. V. Fominov, and Y. Tanaka, *Unconventional Surface Impedance of a Normal-Metal Film Covering a Spin-Triplet Superconductor due to Odd-Frequency Cooper Pairs*, Phys. Rev. Lett. **107**, 087001 (2011).

[15] P. V. Leksin, N. N. Garif'yanov, I. A. Garifullin, Y. V. Fominov, J. Schumann, Y. Krupskaya, V. Kataev, O. G. Schmidt, and B. Büchner, *Evidence for Triplet Superconductivity in a Superconductor-Ferromagnet Spin Valve*, Phys. Rev. Lett. **109**, 057005 (2012); X. L. Wang, A. Di Bernardo, N. Banerjee, A. Wells, F. S. Bergeret, M. G. Blamire, and J. W. A. Robinson, *Giant Triplet Proximity Effect in Superconducting Pseudo Spin Valves with Engineered Anisotropy*, Phys. Rev. B **89**, 140508(R) (2014); N. Banerjee, C. B. Smiet, R. G. J. Smits, A. Ozaeta, F. S. Bergeret, M. G. Blamire, and J. W. A. Robinson, *Evidence for Spin Selectivity of Triplet Pairs in Superconducting Spin Valves*, Nat. Commun. **5**, 3048 (2014); Y. Gu, G. B. Halász, J. W. A. Robinson, and M. G. Blamire, *Large Superconducting Spin Valve Effect and Ultrasmall Exchange Splitting in Epitaxial Rare-Earth-Niobium Trilayers*, Phys. Rev. Lett. **115**, 067201 (2015).

[16] J. W. A. Robinson, J. D. S. Witt, and M. G. Blamire, *Controlled Injection of Spin-Triplet Supercurrents into a Strong Ferromagnet*, Science **329**, 59 (2010); T. Khaire, M. A. Khasawneh, W. P. Pratt, Jr., and N. O. Birge, *Observation of Spin-Triplet Superconductivity in Co-Based Josephson Junctions*, Phys. Rev. Lett. **104**, 137002 (2010); C. Klose, T. S. Khaire, Y. Wang, W. P. Pratt, Jr., N. O. Birge, B. J. McMorran, T. P. Ginley, J. A. Borchers, B. J. Kirby,

B. B. Maranville, and J. Unguris, *Optimization of Spin-Triplet Supercurrent in Ferromagnetic Josephson Junctions*, Phys. Rev. Lett. **108**, 127002 (2012); J. W. A. Robinson, G. B. Halász, A. I. Buzdin, and M. G. Blamire, *Enhanced Supercurrents in Josephson Junctions Containing Nonparallel Ferromagnetic Domains*, Phys. Rev. Lett. **104**, 207001 (2010); E. C. Gingrich, P. Quarterman, Y. Wang, R. Loloee, W. P. Pratt, Jr., and N. O. Birge, *Spin-Triplet Supercurrent in Co/Ni Multilayer Josephson Junctions with Perpendicular Anisotropy*, Phys. Rev. B **86**, 224506 (2012); J. W. A. Robinson, F. Chiodi, M. Egilmez, G. B. Halász, and M. G. Blamire, *Supercurrent Enhancement in Bloch Domain Walls*, Sci. Rep. **2**, 699 (2012); J. W. A. Robinson, N. Banerjee, and M. G. Blamire, *Triplet Pair Correlations and Nonmonotonic Supercurrent Decay with Cr Thickness in Nb/Cr/Fe/Nb Josephson Devices*, Phys. Rev. B **89**, 104505 (2014).

[17] P. SanGiorgio, S. Reymond, M. R. Beasley, J. H. Kwon, and K. Char, *Anomalous Double Peak Structure in Superconductor/Ferromagnet Tunneling Density of States*, Phys. Rev. Lett. **100**, 237002 (2008); I. T. M. Usman, K. A. Yates, J. D. Moore, K. Morrison, V. K. Pecharsky, K. A. Gschneidner, T. Verhagen, J. Aarts, V. I. Zverev, J. W. A. Robinson, J. D. S. Witt, M. G. Blamire, and L. F. Cohen, *Evidence for Spin Mixing in Holmium Thin Film and Crystal Samples*, Phys. Rev. B **83**, 144518 (2011); K. M. Boden, W. P. Pratt, Jr., and N. O. Birge, *Proximity-Induced Density-of-States Oscillations in a Superconductor/Strong-Ferromagnet System*, Phys. Rev. B **84**, 020510(R) (2011); Y. Kalcheim, O. Millo, M. Egilmez, J. W. A. Robinson, and M. G. Blamire, *Evidence for Anisotropic Triplet Superconductor Order Parameter in Half-Metallic Ferromagnetic La0.7Ca0.3Mn3O Proximity Coupled to Superconducting Pr1.85Ce0.15CuO4*, Phys. Rev. B **85**, 104504 (2012); Y. Kalcheim, I. Felner, O. Millo, T. Kirzhner, G. Koren, A. Di Bernardo, M. Egilmez, M. G. Blamire, and J. W. A. Robinson, *Magnetic Field Dependence of the Proximity-Induced Triplet Superconductivity at Ferromagnet/Superconductor Interfaces*, Phys. Rev. B **89**, 180506(R) (2014); Y. Kalcheim, O. Millo, A. Di Bernardo, A. Pal, and J. W. A. Robinson, *Inverse Proximity Effect at Superconductor-Ferromagnet Interfaces: Evidence for Induced Triplet Pairing in the Superconductor*, Phys. Rev. B **92**, 060501(R) (2015); A. Di Bernardo, S. Diesch, Y. Gu, J. Linder, G. Divitini, C. Ducati, E. Scheer, M. G. Blamire, and J. W. A. Robinson, *Signature of Magnetic-Dependent Gapless Odd Frequency States at Superconductor/Ferromagnet Interfaces*, Nat. Commun. **6**, 8053 (2015).

[18] J. D. S. Witt, J. W. A. Robinson, and M. G. Blamire, *Josephson Junctions Incorporating a Conical Magnetic Holmium Interlayer*, Phys. Rev. B **85**, 184526 (2012).

[19] A. Suter, E. Morenzoni, N. Garifianov, R. Khasanov, E. Kirk, H. Luetkens, T. Prokscha, and M. Horisberger, *Observation of Nonexponential Magnetic Penetration Profiles in the Meissner State: A Manifestation of Nonlocal Effects in Superconductors*, Phys. Rev. B **72**, 024506 (2005).

[20] R. F. Kiefl, M. D. Houssain, B. M. Wojek, S. R. Dunsiger, G. D. Morris, T. Prokscha, Z. Salman, J. Baglo, D. A. Bonn, R. Liang, W. N. Hardy, A. Suter, and E. Morenzoni, *Direct Measurement of the London Penetration Depth in* $YBa_2Cu_3O_{6.92}$ *Using Low-Energy* μSR, Phys. Rev. B **81**, 180502(R) (2010).

[21] E. Morenzoni, B. M. Wojek, A. Suter, T. Prokscha, G. Logvenov, and I. Božović, *The Meissner Effect in a Strongly Underdoped Cuprate Above Its Critical Temperature*, Nat. Commun. **2**, 272 (2011).

[22] E. Stilp, A. Suter, T. Prokscha, Z. Salman, E. Morenzoni, H. Keller, C. Katzer, F. Schmidl, and M. Döbeli, *Modifications of the Meissner Screening Profile in* $YBa_2Cu_3O_{7-\delta}$ *Thin Films by Gold Nanoparticles*, Phys. Rev. B **89**, 020510(R) (2014).

[23] M. G. Flokstra, S. J. Ray, S. J. Lister, J. Aarts, H. Luetkens, T. Prokscha, A. Suter, E. Morenzoni, and S. L. Lee, *Measurement of the Spatial Extent of Inverse Proximity in a* Py/Nb/Py *Superconducting Trilayer Using Low-Energy Muon-Spin Rotation*, Phys. Rev. B **89**, 054510 (2014).

[24] See Supplemental Material at http://link.aps.org/supplemental/10.1103/PhysRevX.5.041021 for details on theory and fitting of the LE-μSR measurements, analytical description of the anomalous Meissner response, numerical solution of the Usadel and Maxwell equations, and supplementary figures.

[25] P. Bakule and E. Morenzoni, *Generation and Applications of Slow Polarized Muons*, Contemp. Phys. **45**, 203 (2004).

[26] E. Morenzoni, H. Glückler, T. Prokscha, R. Khasanov, H. Luetkens, M. Birke, E. M. Forgan, Ch. Niedermayer, and M. Pleines, *Implantation Studies of keV Positive Muons in Thin Metallic Layers*, Nucl. Instrum. Methods Phys. Res., Sect. B **192**, 254(2002).

[27] E. Morenzoni (private communication).

[28] P. Bruno and C. Chappert, *Ruderman-Kittel Theory of Oscillatory Interlayer Exchange Coupling*, Phys. Rev. B **46**, 261 (1992).

[29] J. Unguris, R. J. Celotta, and D. T. Pierce, *Oscillatory Exchange Coupling in* Fe/Au/Fe(100), J. Appl. Phys. **75**, 6437 (1994).

[30] H. Luetkens, J. Korecki, E. Morenzoni, T. Prokscha, M. Birke, H. Glückler, R. Khasanov, H. H. Klauss, T. Ślezak, A. Suter, E. M. Forgan, Ch. Niedermayer, and F. J. Litterst, *Observation of the Conduction Electron Spin Polarization in the Ag Spacer of a* Fe/Ag/Fe *Trilayer*, Phys. Rev. Lett. **91**, 017204 (2003).